

# THE LINE BASED TRANSFORMATION MODEL (LBTM): A NEW APPROACH TO THE RECTIFICATION OF HIGH-RESOLUTION SATELLITE IMAGERY

Ahmed Shaker

Department of Land Surveying and Geo-Informatics, The Hong Kong Polytechnic University, Hong Kong  
[a.shaker@polyu.edu.hk](mailto:a.shaker@polyu.edu.hk)

**KEY WORDS:** Remote Sensing, Geometry, Correction, Rectification, Georeferencing, Imagery, Model, High-resolution

## ABSTRACT:

For various satellite imagery applications, geo-referencing through rectification is a common operation. Rigorous mathematical models with the aid of satellite ephemeris data can present the relationship between the image space and object space. With government funded satellites, access to calibration and ephemeris data allowed the development of these models. However, for commercial high-resolution satellites, these data have been withheld from users, and therefore alternative empirical rectification models have been developed. In general, most of these models are based on the use of control points. The lack of control points in some remote areas such as deserts, forests and mountainous areas provides a catalyst for the development of algorithms based on other image features. One of the alternatives is to use linear features obtained from scanning/digitizing hardcopy maps, from terrestrial mobile mapping systems or from digital images.

In this work, a new model named the Line Based Transformation Model (LBTM) is established for satellite imagery rectification. The model has the flexibility to either solely use linear features or use linear features and a number of control points to define the image transformation parameters. As with other empirical models, the LBTM does not require any sensor calibration or satellite ephemeris data. The underlying principle of the model is that the relationship between line segments of straight lines in the image space and the object space can be expressed by affine or conformal relationships. Synthetic as well as real data have been used to check the validity and fidelity of the model, and the results show that the LBTM performs to a level comparable with existing point based transformation models.

## 1. INTRODUCTION

Point feature based transformation models have been, for several decades, used extensively in photogrammetry and remote sensing for image rectification and terrain modeling. They are driven by linking points in the image space and the corresponding points in the object space using rigorous mathematical models. However, under many circumstances accurately identifying discrete conjugate points may not be possible. Unlike point features, which must be explicitly defined, linear features have the advantage that they can be implicitly defined by any segment along the line. In the era of digital imagery, linear features can be easily identified in the image by many automatic extraction tools and in object space, they can be obtained from an existing GIS database, hardcopy maps, and terrestrial mobile mapping systems (using for instance kinematic GPS techniques). Therefore, using linear features becomes an advantage, especially because they add more information, increase redundancy, and improve the geometric strength of adjustment (Habib et al, 2003). Some effort has been made to use linear features in photogrammetric applications for frame and linear array scanners. However, some of these techniques use linear features as constraints and are still based on rigorous mathematical models, which need all sensor model information.

Mulawa and Mikhail (1988) present the concept of linear features in photogrammetric tasks in which linear features and photogrammetric observations are combined in the formulation. Kanok (1995) and Mikhail and Kanok (1997) have used an independent set of linear feature descriptors to present the relationship between image space and object space. The method is based on the observation that any ray from the perspective

center passing through a point on the image line must intersect the object line. In their approach, the standard point-based photogrammetric collinearity equations were replaced by line-circle based ones. Instead of the regularly used two collinearity equations, a single equation is established to ensure the coplanarity of a unit vector defining the object space line, the vector from the perspective center to a point on the object line, and the vector from the perspective center to a point on the image line. Furthermore, coordinate transformations are implemented on the basis of linear features. In this case, feature descriptors are related instead of point coordinates.

Further work has been done to accommodate linear features for single photo resection and automatic relative orientation. Habib et al (2002 and 2003) have suggested an algorithm to solve the problems relating to the correspondence between image and object space lines. This matching problem is solved through a modified version of the generalized Hough transform. The work introduced algorithms to incorporate straight lines into aerial triangulation for frame and linear array scanner imagery. The collinearity condition is used in single photo resection to present the relationship between matching entities in image and object space and the coplanarity condition is used in case of automatic relative orientation. This work suggests that linear features can be used to provide constraints in photogrammetric applications.

In the absence of sensor calibration and satellite orbit information, there are several limitations in applying such techniques to High Resolution Satellite Imagery (HRSI): a) all those presented are based on rigorous mathematical models which require sensor and system parameters that are withheld from the HRSI user community; b) when using linear features,

rather than point features, conventional photogrammetric rules may not be appropriate (Mikhail and Kanok, 1994); c) most of these models are valid for the projective geometry imagery of a photograph which is not exactly the case for linear array sensor imagery; d) the models become quite complicated when modified for the geometry and time dependency characteristics of linear array scanners; e) numerical problems could be encountered because of the initial approximation; and finally, f) constraints improve accuracy of the adjustment and increase the redundancy in estimation but each constraint adds an additional parameter to the adjustment and multiple constraints may lead to over parameterization (Habib et al., 2003).

To date, there has been a substantial body of work dealing with non-rigorous mathematical models (such as rational functions, affine, polynomial, and DLT models) to circumvent the absence of satellite information and to rectify HRSI (see for example Fraser et al. (2002), Fraser and Hanley (2003), Shi and Shaker (2003), and Grodecki and Dial (2003)). These models are point based and have focused on two main aspects concerning accuracy: the accuracy attainable in image rectification, and the accuracy of DTM extraction by stereo spatial intersection. All reports demonstrate that the models described in them produce acceptable results.

It is obvious that linear features can be used with rigorous mathematical models and points can be applied to non-rigorous mathematical models. That leads to the question of "Can linear features be used with non-rigorous mathematical models in order to circumvent the absence of satellite information and maintain satisfactory results?" This research answers the question with the development of a new model named the Line Based Transformation Model (LBTM).

With the LBTM, most of the problems of using linear features with the present generation of rigorous models have been overcome. The model can either solely use linear features or use linear features plus a number of control points to define the image transformation parameters. It is a very simple model which is time independent, can be applied to images from any linear array sensor, does not require any information about sensor calibration or satellite orbit, and does not require any initial approximation values. The underlying principle of the model is that the relationship between line segments of straight lines in the image space and the object space can be expressed by affine or conformal relationships. The model adopts the same structure for 3D transformation as the eight-parameter affine model, and the same structure for 2D transformation as the six-parameter affine and four-parameter conformal models. Adopting these structures further allowed direct comparison between the developed LBTM and the existing models. Synthetic as well as real data have been used to check the validity and fidelity of the model and the results show that the LBTM can be used to efficiently and accurately rectify HRSI.

## 2. THE MATHEMATICAL MODEL

Successful exploitation of linear features in image rectification and terrain modeling requires consideration of the following two major aspects: the mathematical description of linear features in image and object space and the mathematical representation of the relationship between the two spaces. There are different options for representing linear features in both image and object space. Straight lines, circles, ellipses and free form lines are examples of such representation. In this work, straight lines as well as natural lines (free form lines) converted

to straight lines by mathematical functions are used. Circles and ellipses are discarded due to their impracticality and because they are not transformation invariant.

Various forms of equations can represent straight lines in two and three-dimensional spaces with each of them exhibiting some weakness in certain applications. For each of these forms, describing a line in 2D or 3D space requires two or four independent parameters, respectively. Straight lines can be represented in either image or object space in different ways such as the intersection between two planes, line descriptors, unit vectors and normal to line descriptors. The Line Based Transformation Model (LBTM) is based on the relationship between the unit vector components of a line in image space and the unit vector components of the conjugate line in object space. Unit vector representation, which can be obtained from any two points along straight line segments, was chosen because they can be easily defined from images, existing geodatabases or terrestrial mobile mapping systems in both image and object space. However, the unit vector is not a unique representation of a straight line as it can represent the line in question and an infinite number of parallel lines. This problem is addressed in section 2.1.1.

The LBTM applies to high-resolution satellite imagery produced from CCD linear array sensors, which are widely used in remote sensing applications. Regardless of the capturing technique (cross or along track), images from linear array sensors consist of independent scanned lines. Each line on the image is the result of a nearly parallel projection in the flight direction and a perspective projection in the CCD line direction. Therefore, rigorous mathematical models based on the collinearity equations and including a time dependent function could be applied for geo-referencing the images. To circumvent the complexity of the time dependent model, in other words, to simplify the relationship between image and object coordinate systems, several assumptions were adopted: (a) the satellite sensor moves linearly in space with stable attitude; (b) the sensor orientation angles are constant; and (c) the satellite flight path is almost straight.

Under these assumptions, the scanned lines from the sensor can be considered to form a continuous (single) image. These characteristics allow the ordinary collinearity equations between the satellite imagery and the ground to be replaced by simple affine and conformal transformation models similar to those introduced in Hanly and Fraser (2001) and Fraser et al., (2002). The underlying principle of the developed model is that the unit vector components in either image or object space could replace the point coordinates in the previous models. Both affine and conformal implementations of the LBTM were developed. The derivation of the 3D affine LBTM is given in the following section and the 2D affine and the 2D conformal LBTM form can be obtained by simplification. Here we will refer to eight-parameter affine model, six-parameter affine model, and four-parameter conformal model as 3D affine model, 2D affine model and 2D conformal model respectively.

### 2.1 The 3D affine LBTM

Vectors  $\bar{v}_{12}$  and  $\bar{V}_{12}$  are unit vectors for conjugate lines in image and object space respectively (see Figure 1). The two unit vectors can be defined by any two points along the line segment in image and object space. Suppose that point  $p_1 = (x_1, y_1)$  and

$p_2 = (x_2, y_2)$  are two points on the line in image space, then  $\vec{v}_{12}$  can be presented in matrix form as:

$$\vec{v}_{12} = [a_x \quad a_y \quad 0]^T \quad (1)$$

where:

$$a_x = \frac{x_2 - x_1}{\sqrt{(x_2 - x_1)^2 + (y_2 - y_1)^2}} \quad \text{and} \quad a_y = \frac{y_2 - y_1}{\sqrt{(x_2 - x_1)^2 + (y_2 - y_1)^2}}$$

On the other hand, suppose that points  $P_1 = (X_1, Y_1, Z_1)$  and  $P_2 = (X_2, Y_2, Z_2)$  are located on the conjugate line in the object space. Then, the unit vector  $\vec{V}_{12}$  is:

$$\vec{V}_{12} = [A_x \quad A_y \quad A_z]^T \quad (2)$$

where:

$$A_x = \frac{(X_2 - X_1)}{\sqrt{(X_2 - X_1)^2 + (Y_2 - Y_1)^2 + (Z_2 - Z_1)^2}}$$

$$A_y = \frac{(Y_2 - Y_1)}{\sqrt{(X_2 - X_1)^2 + (Y_2 - Y_1)^2 + (Z_2 - Z_1)^2}}$$

$$A_z = \frac{(Z_2 - Z_1)}{\sqrt{(X_2 - X_1)^2 + (Y_2 - Y_1)^2 + (Z_2 - Z_1)^2}}$$

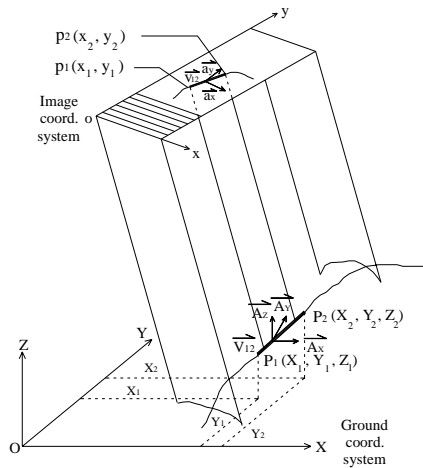


Figure 1 Unit line vector representation in image and object space (case of linear array sensor).

It is worth mentioning that points  $p_1, p_2$  and  $P_1, P_2$  in image and object spaces are not conjugate points, but the lines they lie on are conjugate lines. As was mentioned earlier, the relationship between image and object space can be represented by 3D affine transformation for HRSI. The same relationship between the two coordinate systems is used to represent the relationship between vectors in image and object space. Any vector in object space can be transformed into its conjugate vector in image space by applying rotation, scale, and translation parameters as shown in equation (3):

$$\vec{v} = M\lambda\vec{V} + T \quad (3)$$

where  $\vec{v}$  and  $\vec{V}$  are vectors of line segment in image and object space respectively,  $M$  is a rotation matrix relating the two coordinate systems,  $\lambda$  is a scale matrix (a diagonal matrix providing different scales in different directions), and  $T$  is a translation matrix.

The elements of  $M$  are functions of three sequential rotations about the X, Y and Z (object) coordinate axes and are the same as used in the derivation of the collinearity equations used in photogrammetry. Substituting the various presented matrices into equation 3 gives:

$$\begin{bmatrix} a_x \\ a_y \\ 0 \end{bmatrix} = \begin{bmatrix} m_{11} & m_{12} & m_{13} \\ m_{21} & m_{22} & m_{23} \\ m_{31} & m_{32} & m_{33} \end{bmatrix} \begin{bmatrix} \lambda_1 & 0 & 0 \\ 0 & \lambda_2 & 0 \\ 0 & 0 & \lambda_3 \end{bmatrix} \begin{bmatrix} A_x \\ A_y \\ A_z \end{bmatrix} + \begin{bmatrix} T_x \\ T_y \\ T_z \end{bmatrix} \quad (4)$$

where  $\lambda_1, \lambda_2, \lambda_3$  are scale factors,  $m_{11}, m_{12}, \dots, m_{33}$  are the rotation matrix elements,  $(a_x, a_y)$  are the line unit vector components in the image space coordinate system,  $(A_x, A_y, A_z)$  are the line unit vector components in the object space coordinate system, and  $T_x, T_y, T_z$  are the components of the translation matrix between the image and the object coordinate systems in X, Y and Z directions. The previous form is valid only if the scale factor is equal to  $\pm 1$  since the transformed vectors, in this case, are unit vectors. This condition is necessary and should be sufficient to validate the equation. Then, the equation will lead to the following individual equations

$$a_x = (\lambda_1 m_{11} A_x + \lambda_2 m_{12} A_y + \lambda_3 m_{13} A_z) + T_x \quad (5)$$

$$a_y = (\lambda_1 m_{21} A_x + \lambda_2 m_{22} A_y + \lambda_3 m_{23} A_z) + T_y \quad (6)$$

$$0 = (\lambda_1 m_{31} A_x + \lambda_2 m_{32} A_y + \lambda_3 m_{33} A_z) + T_z \quad (7)$$

After substituting the scale factors  $\lambda_i$  multiplied by the rotation matrix coefficients  $m_{iv}$ , and the translation components  $T_{x-z}$ , by the new coefficients  $b_i$ , the transformation equation can be rewritten as:

$$a_x = b_1 A_x + b_2 A_y + b_3 A_z + b_4 \quad (8)$$

$$a_y = b_5 A_x + b_6 A_y + b_7 A_z + b_8 \quad (9)$$

where  $b_1$  to  $b_3$  and  $b_5$  to  $b_7$  present the rotation and scale factors, and  $b_4, b_8$  are translation coefficients. Equations 8 and 9 represent the mathematical form of the 3D affine LBTM.

The model is similar to the ordinary 3D affine model used by Fraser et al. (2002), with the only difference being the use of line unit vector components instead of point coordinates in order to calculate the model coefficients (image parameters). A unique solution for the new model coefficients could be calculated by using four Ground Control Lines (GCLs), which are conjugate image/object lines. If the number of observations available (number of GCLs) is more than the minimum amount, then a least squares adjustment is used.

**2.2.1 The unit vector problem:** As mentioned above, unit vectors do not provide a unique representation of a line and thus the LBTM expresses the relationship between a group of lines in image space and any other parallel group of lines in object space. Comparing the coefficient values calculated from the test data with the use of the ordinary 3D affine model and GCPs with the coefficient values calculated with the use of the developed 3D affine LBTM and control lines (unit vector components) shows: a) very small differences between those coefficients representing rotation and scale factors; b) large differences between the translation coefficients. This finding suggests that there is a problem in the LBTM concerning calculation of translation coefficients.

Several solutions can be applied to overcome this problem. First, the translation coefficients may be recovered if the shift between the origins of the two coordinate systems is known. In this case, the six coefficients representing the scale and rotation are recovered by the aid of the GCLs and then the translation coefficients ( $b_4$  and  $b_8$ ) will be determined from the shift between the origins. This is a special case, which occurs only when local image and object coordinate systems are used. Second, the six coefficients relating the scale and rotation transformation coefficients are recovered as in the first case and a single GCP could be used to define the translation coefficients.

**2.1.2 Using the 3D affine LBTM:** Similar to the collinearity equations in photogrammetry, the 3D affine LBTM can be applied to various operations such as space resection for calculating the model coefficients (image parameters), space intersection for determining the location of a 3D point, and image rectification. Recovering the model coefficients for images by the LBTM leads to one of the followings processes: either working on 2D image rectification (in case of single image transformation) or 3D geo-positioning determination (in case of using stereo pair images). For image rectification, points in image space could be transferred directly to an object plane by assuming an average elevation of terrain for the whole area covered by the image and by using the recovered model coefficients and image coordinates of the points. For the same purpose, a Digital Elevation Model (DEM) could also be used together with the previous information to enhance the results, especially when the model is applied to undulated terrain.

For 3D geo-positioning determination, stereo images should be used. More specifically, a group of GCLs should be used to recover the stereo image parameters individually and then 3D point coordinates could be calculated. Each point in the area covered by the stereo images will raise four equations to recover the three unknowns (X,Y,Z), which means one redundancy is available to check the quality of the results.

## 2.2 The 2D LBTM

Two-dimensional transformations are required in many applications of photogrammetry and remote sensing. We often need to convert between coordinates in two different plane systems having different origins, orientations, and possibly scales. More importance is added to the need for a 2D transformation when terrain information is either not necessary (as in case of flat terrain or low accuracy requirements) or not available (as in case of remote, unmapped areas).

Similar to the way in which point coordinates in the 3D affine LBTM are replaced with unit vectors, the 2D affine LBTM can be rewritten as follows:

$$a_x = C_1 A_x + C_2 A_y + C_3 \quad (10)$$

$$a_y = C_4 A_x + C_5 A_y + C_6 \quad (11)$$

where ( $a_x, a_y$ ) are unit vector components of a line segment in the image coordinate system, ( $A_x, A_y$ ) are planimetric unit vector components of the conjugate line segment in the object coordinate system, and  $C_1, \dots, C_6$  are the model coefficients.

In addition, the 2D conformal LBTM can be presented for unique scale transformation as follows:

$$a_x = C_1 A_x - C_2 A_y + C_3 \quad (12)$$

$$a_y = C_2 A_x + C_1 A_y + C_4 \quad (13)$$

where ( $a_x, a_y$ ) and ( $A_x, A_y$ ) are unit vector components of the line segment in the image and object coordinate system respectively, and  $C_1, \dots, C_4$  are the model coefficients.

As was demonstrated in the derivation section of the 3D affine LBTM, line unit vectors are not a unique representation of lines. Therefore, coefficients presenting the scale and rotation can be recovered with the use of GCLs (as was explained in section 2.1.1), and calculating the translation coefficients will require one additional GCP. A minimum of three GCLs is sufficient for the determination of the 2D affine LBTM coefficients, and a minimum of two GCLs is enough to calculate the 2D conformal LBTM coefficients. Comparing the 3D LBTM to the 2D LBTM, it can be said that the latter can be applied to rectify single images instead of stereo images without needing any relief related information. As with the 3D LBTM, synthetic as well as real data have been used to verify the 2D LBTM model and the results are presented in the following section.

## 3. EXPERIMENTAL RESULTS AND ANALYSIS

### 3.1 Synthetic Data

The effects of various factors such as differences in terrain elevation, inclination angle, length, number, and distribution of GCLs were tested for the developed model. Image coordinates of four sets (S1, S2, S3, S4) of synthetic stereo image data were derived from the actual orientation parameters of a stereo pair of Ikonos imagery and synthetic object coordinates of 48 well-distributed points. The sets were derived so that both S1 and S3 represented undulating terrain with height variations of about 100 m, while S2 and S4 represented flat terrain with height variations of less than 15 meters.

Two different configurations of 12 GCLs were established from half of the object points and the remaining object points were used as checkpoints. One configuration consisted of long, 200 – 500 meter, lines with random orientations and the other of short, 100 – 200 meter, lines predominately aligned to the diagonals of the image. S1 and S2 used the long lines, while S3 and S4 used the short lines. The two configurations of GCLs and checkpoint data are shown in Figures 2 and 3 respectively.

Extensive sets of experiments were performed, but only a few representative cases are reported here due to the space limitations. Tables 1 and 2 present the results of the 3D and 2D affine LBTM respectively. Different groups of GCLs (from 4 to 12 GCLs) plus one additional GCP were used, and the results are summarized in terms of RMS errors of the 24 independent checkpoints in the X and Y directions. The RMS errors in the Z direction (in case of using the 3D affine LBTM) are not considered here as this study focuses on the rectification of the satellite imagery. A detailed discussion of the 3D geo-positioning determination will be presented in a future publication.

From the results obtained, it is obvious that the LBTM works significantly well for image rectification. The investigation shows that, except for the translation coefficients which are calculated by the aid of the additional GCP, coefficients

calculated by the LBTM are almost identical to those obtained from the ordinary 3D/2D affine models and GCPs. Applying different configurations of the control straight lines indicates that the inclination angle (the angle in the XY plane) of the control line does not affect significantly the accuracy of the results but the distribution of the GCLs on the area covered by the image does. Increasing the number of GCLs improves the accuracy of the results; however, a key feature established from these results is that the GCL slope, which is a function of the GCL length and terrain elevation differences along the line, has the most important effect on the results accuracy. The results presented below are chosen to illustrate this phenomenon.

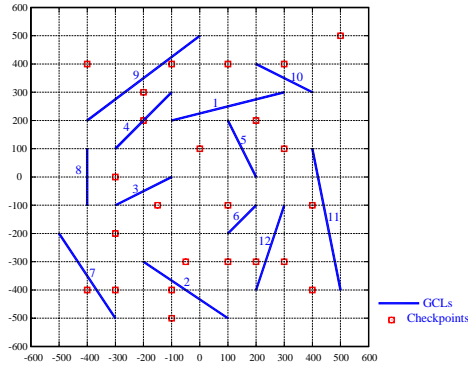


Figure 2. GCLs and checkpoints distribution of S1 and S2 sets

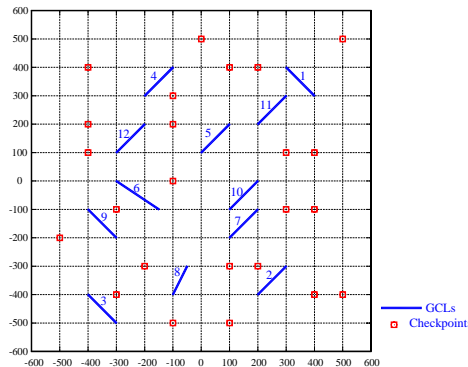


Figure 3. GCLs and checkpoints distribution of S3 and S4 sets

| Data Set  |         | No. of GCLs | No. of Chkpts | The 3D affine LBTM |            |
|-----------|---------|-------------|---------------|--------------------|------------|
|           |         |             |               | Total RMS (m)      |            |
|           |         |             |               | X                  | Y          |
| Synthetic | Case S1 | 4-12        | 24            | 5.32- 2.92         | 2.04- 2.26 |
|           | Case S2 |             |               | 0.20- 0.21         | 0.29- 0.23 |
|           | Case S3 |             |               | 4.32- 3.27         | 4.21- 2.62 |
|           | Case S4 |             |               | 2.03- 1.47         | 1.84- 1.67 |
| Real (HK) |         | 4-12        | 16            | 9.01- 2.39         | 6.96- 2.01 |

Table 1: The 3D affine LBTM results of the synthetic and the real data

| Data Set  |         | No. of GCLs | No. of Chkpts | The 2D affine LBTM |            |
|-----------|---------|-------------|---------------|--------------------|------------|
|           |         |             |               | Total RMS (m)      |            |
|           |         |             |               | X                  | Y          |
| Synthetic | Case S1 | 4-12        | 24            | 3.81- 3.01         | 6.99- 4.60 |
|           | Case S2 |             |               | 0.46- 0.28         | 1.10- 0.51 |
|           | Case S3 |             |               | 3.96- 2.17         | 5.77- 6.31 |
|           | Case S4 |             |               | 3.76- 1.49         | 1.63- 0.46 |
| Real (HK) |         | 4-12        | 16            | 7.73- 5.09         | 8.19- 9.14 |

Table 2: The 2D affine LBTM results of the synthetic and the real data

When considering the effect of the terrain type, the results in Table 1 indicate that data set S2 (flat terrain) yields more accurate results than data set S1 (undulated terrain) in all directions, the same way as data set S4 leads to more accurate results than data set S3. The results also show that the sharper the slopes of GCLs are, less accurate the results are. Applying the 2D affine LBTM to the same data sets leads to similar findings; however, the overall accuracy is generally worse than when using the 3D affine LBTM. The deficit of the results is especially clear when applying the 2D affine LBTM to the sets of the undulated terrain. This finding is expected because the 2D LBTM does not consider the differences in terrain elevation. On the basis of the above, one can conclude that the selection of the LBTM form to be used for image rectification depends primarily on terrain elevation differences. In the following section a real data set is used to examine the feasibility and the performance of the developed model.

### 3.2 Real Data

To verify the results obtained from the simulated data, a real stereo data set (Ikonos Hong Kong data set) was used. The area covered by the two images extends over 11.60 x 10.28 km<sup>2</sup> for image 1 and 6.62 x 10.18 km<sup>2</sup> for image 2 of the stereo with the overlap area of 2.5 x 10 km<sup>2</sup>. The inclination angles of the images are 19.02 and 27.3 degrees respectively, which leads to the base to height (B/H) ratio of about 0.87. The maximum ground elevation difference in the test area is about 450 meters. A fast static GPS technique was used to collect thirty-eight well-distributed GCPs on the entire coverage area of the two images; among them, eighteen GCPs belong to the overlap area. Most of the observed points were road intersections, pavement corners, or road-canal intersections. Further information about the test field can be found in Shi and Shaker, 2003 and Shaker et al., 2004.

A number of GCLs were established by connecting different points in the overlap area between the two images and the 3D LBTM was applied. The results show that the new model is applicable to the real data, though solid conclusions could not be drawn as the data set had limited overlap coverage area (2.5x10 km<sup>2</sup>) and dependent checkpoints (the same 18 points which are used to establish the GCLs). Consequently, the coverage area of image 2 of the data set (6.62 x 10.18 km<sup>2</sup>) was extended to cover the same area as in image 1 (11.60 x 10.28 km<sup>2</sup>). The image coordinates of the extension area of image 2 were calculated by using the ground coordinates of the observed GPS points, the corresponding image coordinates of image 1, and the ordinary affine model parameters as they defined in Shi and Shaker, 2003. Accordingly, the two image coordinates and the object coordinates of a set of the 38 points were ready for the experiment.

After several attempts to generate control straight lines, a group of 12 GCLs were established by connecting some of the GCPs of the data set keeping in mind that the lines were matching real linear features such as roads or canals. The remaining points were used as checkpoints (16 independent checkpoints). The final distribution of GCLs and checkpoints used in this investigation are presented in Figure 4.

The accuracy of the results of applying the established GCLs plus one additional GCP to the developed LBTM was found to be matching the accuracies which resulted from using the simulated data. It is important to mention that the data set did not contain any high slope GCL; however, the GCLs comprising in the data set presented different levels. Tables 1

and 2 show the results for the cases of using the 3D and 2D affine LBTMs, respectively. The results reveal that the accuracy level of about 2 m in X and Y directions can be achieved by applying 12 GCLs to the 3D affine LBTM. However, the accuracy declined to about 5 m in X and 9 m in Y when using the 2D affine LBTM and the same number of GCLs. This last finding is consistent with our expectations and the results obtained from applying the 2D affine LBTM to the simulated data because the effects of the terrain elevation differences (about 450 m in this study area) are not considered. In this case, the results in the X direction are better than the results in the Y direction (when using the 2D affine LBTM) because of the along track capturing techniques. In general, the results are comparable to what was achieved by using the 3D affine model and GCPs in Shi and Shaker, 2003. In addition, the results suggest that the developed LBTM is applicable to and reveals an accurate performance for high-resolution satellite imagery rectification.

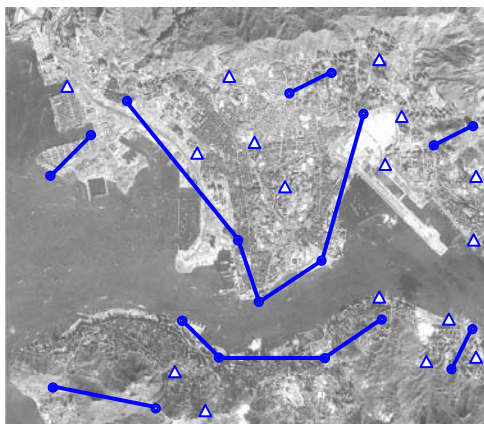


Figure 4. GCLs and checkpoints distribution of the Hong Kong data set.

#### 4. CONCLUSIONS AND FURTHER WORK

The Line Based Transformation Model is proposed for the rectification of high-resolution satellite imagery. This is an attempt to establish a new model, which can deal with linear features and/or linear features with a number of GCPs. In this model, most of the problems encountered in previous models using linear features have been overcome. In addition, sensor calibration and satellite orbit information, which are withheld from the user community for most of the new high-resolution satellites, are not required.

The underlying principle of the new model is that the line unit vector components of a line segment could replace the point coordinates in the representation of the ordinary 3D/2D affine and conformal models. Any two points along a line segment could be measured in image and object spaces to calculate the line unit vector. It is noteworthy that the two line segments in image and object spaces are not required to be the same, but are required to be segments of conjugate lines. Experiments with synthetic and real data have been conducted and the results prove the applicability of the new model for image rectification. The analysis of the results obtained from the LBTM indicates that the slope values of GCLs, which are based on the differences in terrain elevations along the line and the line length, significantly affect the accuracy of the results. The lower the slopes of GCLs are, the higher accuracy can be

attained, and visa versa. No significant differences in the results could be recorded for flat terrain.

Currently, the applicability of the developed model for the rectification of images produced by several high-resolution satellites such as IRS-1D, SPOT-5 and QuickBird is under study. In addition, the effects of the sensor inclination angles on the performance of the model and possible limitations of the model are examined. Finally, we are also investigating the possibility of extending the use of the new model for frame cameras.

#### ACKNOWLEDGMENTS

This project is fully supported by the Hong Kong Polytechnic University (project no. G-W129). The Ikonos image for Hong Kong used in this study is from CERG project 'Optimum Compression of One-Meter Satellite Images for mapping purposes.' The author would like to acknowledge Dr. Bruce King for his invaluable contributions to the work. He also expresses his gratitude to Dr. John Shi.

#### REFERENCES

- Fraser, C.S., Hanely, H.B., 2003. Bias compensation in rational functions for Ikonos satellite imagery. *Photogrammetric Engineering and Remote Sensing (PE&RS)*, 69(1), pp. 53-57
- Grodecki, J., and Dial, G., 2003. Block adjustment of high-resolution satellite images described by rational polynomials. *PE&RS*, 69(1), pp. 59-68
- Habib, A., Morgan, M., and Lee, Y. R., 2002, Bundle adjustment with self-calibration using straight lines. *Photogrammetric Record*, 17(100), pp. 635-650.
- Habib, A.F., Lin, H.T., and Morgan, M.F., 2003. Line-based modified iterated Hough transform for autonomous single-photo resection. *PE&RS*, 69(12), pp. 1351-1357
- Hanly, H.B., and Fraser, C.S., 2001. Geopositioning accuracy of Ikonos imagery: Indications from two dimensional transformations. *The Photogrammetric record*, 17(98), pp. 317-329
- Kanok, W., 1995. Exploitation of linear features for object reconstruction in digital photogrammetric systems. PhD thesis, Purdue University.
- Mikhail, E. M., and Kanok, W., 1994. Feature-based photogrammetric object construction. *ASPRS/ACSM annual conference*, Reno, Nevada, pp. 403-417.
- Mikhail, E.M., and Kanok, W., 1997. Exploitation of linear features in surveying and photogrammetry. *Journal of surveying engineering*, 123(1), pp. 32-47.
- Mulawa, D. C., and Mikhail, E. M., 1988. Photogrammetric treatment of linear features. *ISPRS 16th congress, Commission III*, 27(part B10), pp. 383-393, ISPRS, Elsevier, Amsterdam, The Netherlands.
- Shaker, A., and Shi, W. Z., 2003. "Polynomial models as a tool for mapping high-resolution satellite imagery", *European remote sensing conference (SPIE)*, Barcelona, Spain, on CD.